Combined Experimental and Theoretical Analysis of the Mixed Mode Bending Test

N. Ben Salem[1,2,3], J. Jumel[1,2,3,*], M.K. Budzik[1,2,3], M.E.R. Shanahan[1,2,3]

[1] Université de Bordeaux, I2M, UMR 5295, F-33400 Talence, France
[2] CNRS, I2M, UMR 5295, F-33400 Talence, France
[3] Arts et Metiers ParisTech, I2M, UMR 5295, F-33400 Talence, France
* Corresponding author, 351 cours de la libération, 33405 Talence Cedex ,France

ABSTRACT. *A crack propagation test is performed under mixed mode I and mode II condition along the interface of an aluminium/aluminium joint bonded with EA9321© epoxy paste using a Mixed Mode Bending (MMB) apparatus. Supplementary instrumentation is added to the system for a finer test control but also for a precise probing of the cohesive forces distribution in the adhesive at the vicinity of the crack tip. In Addition to the usual load cell and displacement sensors which are used for measuring the applied force and specimen mid-span deflection and opening, Digital Image Correlation technique is used for full field observation of the specimen deformation near the crack tip position. Finally, backface strain monitoring technique is used to probe with a high sensitivity the presence of cohesive force gradient near the crack tip. All the experimental results are compared with the one obtained with a simple model consisting of two Timoshenko Beams bonded with an elastic interface. Satisfying agreement between theoretically and experimentally determined displacement fields which indicates that such measurement should allow the evaluation of effective stiffness. On the contrary, backface strain monitoring measurements evidence significant difference between the two which indicates that this technique should enable a finer characterization of the non linear behaviour of the adhesive layer.*

INTRODUCTION

Fracture mechanic and damage tolerance methods have proven to allow conservative but reliable approach for designing bonded assemblies and/or composite structures. Indeed, these parts often suffer from geometric or material discontinuities which produce stress singularities from which crack can initiate and propagate [1]. The crack initiation and propagation resistance is generally controlled by the critical energy release rate which was originally characterized in bonded joint under mode I condition with the Double Cantilever Beam test [2]. Since then, a large number of experimental configurations have been proposed to evaluate the fracture resistance of interfaces under more complex loading conditions (mixed mode [3], unstationnary loading [4] ...).

Besides, cohesive zone models have been introduced to improve the description of the interface behaviour and damage when under such complex loading [5,6]. However, these models suffer from a lack of efficient experiment technique for a precise identification of the interface separation laws which are mainly identified from macroscopic force versus displacement measurements [7]. Recently, a method based on the simultaneous measurement of the J integral and crack tip opening displacement $J(\delta)$ has been developed [8] for simple derivation of the interface separation law which has been also applied under mixed mode loading conditions [9,10]. Finally, Backface strain monitoring has proven recently a high sensivity for probing the presence of cohesive force gradient in the bondline at the vicinity of the crack tip. This technique has been applied to study mode I [11], mode II [12] and mode III [13] crack propagation, but has not been used in a standardized mixed I/II mode configuration such as with the MMB test.

In the present article, a crack initiation and propagation experiment is performed on an adhesively bonded joint made with two aluminium adherends using a toughen epoxy paste. The usual experimental data reduction techniques are used together with Digital Image Correlation Analysis and backface strain monitoring technique to achieve proper mode I and mode II contribution separation but also for fine probing of the shear and peel stress distribution in the vicinity of the crack tip.

MATERIALS AND TEST PROCEDURE

Specimen preparation

The specimen is made with two aluminium (AW7075-T6) adherends bonded with Hysol®EA9321 epoxy paste. t = 5mm adherend thickness is chosen to prevent from any irreversible strain in the adherend during the experiment. Others dimensions are, width w = 12 mm and total length 200 mm. The specimen is hold in the MMB apparatus through end blocks which are directly machined in each adherend. Prior bonding, the bonded surfaces are grit-blasted using 200µm grain-size Al_2O_3 particles then immersed in ethanol in an ultrasonic bath, rinced in acetone and finally dried with a hot air gun. Subsequently, the aluminium is anodized using PAA treatment, following ASTM D3933 recommendation. Finally, a 1% solution of 3-mercaptopropyltrimethoxy silane in deionised water in deposited at on the surfaces to be bonded as adhesion promoter. The adherends are heated at 92°C during 1 hour in a furnace to allow solvent evaporation.

The hysol EA9321® is a two part epoxy system. The resin is derived from bisphenol A and contains fumed silica particles. It is mixed manualy with TEPA (triethylenepentamine) curing agent following the resin to hardener weight ratio indicated in the supplier's documentation (100:17). The two component are mixed manually with a spatula until a uniform aspect is observed. However, at a microscopic scale, a large number of voids are observed which are uniformly distributed both spatially and in size.

The adherends are then placed in alignment tools and the adhesive paste is manually deposited. PTFE spacers are placed at both ends of the specimen and both parts are pressed together under 1MPa pressure so that uniform bondline thickness (350µm) is obtained. The specimen is left at ambient temperature during 12 hours for crosslinking. Then crosslinking is achieve by heating the specimen in a furnance during 90 min at 82°C following supplier's documentation. Dynamical Mechanical Analysis indicates that the glass temperature transition of the adhesive is *ca.* 120°C. Prior testing, a sharp crack is created by forcing a wedge in between the two adherends. The crack propagation is stopped with a clamping collar, the initial crack length is a_0 = 50mm.

Fracture energy measurement and instrumentation

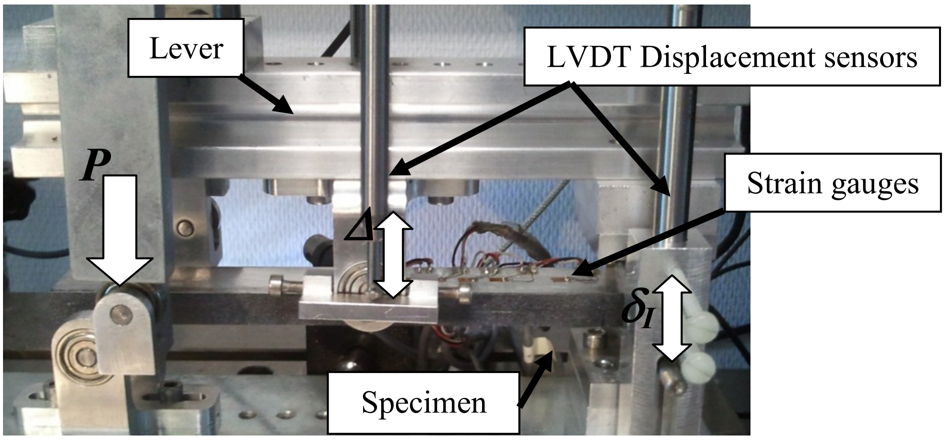

Figure 1. Description of the instrumented MMB test experimental set-up.

The MMB apparatus used for the mixed mode I/II fracture test is similar to the one recommended by the standard ASTM D5528 (see Figure 1). To minimize the need for geometrical correction due to the lever rotation. Two LVDT displacement sensors with 20mm range are added to measure the specimen opening δ_I associated to the mode I contribution so the deflection at the mid-span position Δ. From these two measurements the mode II contribution is determined with the relation $\delta_{II} = \delta_I/4-\Delta$.
Similarly, with a simple static equillibrium analysis of the lever the partition of the applied force into mode I, P_I, and mode II, P_{II}, loads is easliy found. Classically, we find :

$$P_I = \frac{3c-L}{4L}P \qquad\qquad P_{II} = \frac{3c-L}{4L}P \tag{1}$$

where L = 90mm is the mid-span length and c is the distance between the mid-span and the position where the tensile testing machine (Zwick/Roell Z010, Zwick GmbH & Co., Ulm, Germany) applies the load on the lever. A 10KN load cell (Zwick/Roell, KAF-TC) is used the measure the compression force on the lever. The test is performed under constant crosshead displacement speed 0.3 mm.min^{-1} at ambient temperature *ca.* 23°C. In the most simple analysis of the MMB test is a direct application of the Linear Elastic Fracture Mechanics, the system is considered as elastic, the adherends are modeled as beam in bending so that the MMB test can be considered as a simple superposition of the Double Cantilever Beam and the 3 points bending End Notched Flexure tests. The compliance of DCB and 3-ENF specimens are given by the following relations :

$$C_I = \frac{\delta_I}{P_I} = \frac{8a^3}{Ewt^3} + \frac{2a}{\kappa Gwt} \qquad C_{II} = \frac{\delta_{II}}{P_{II}} = \frac{3a^3 + 2L^3}{8Ewt^3} + \frac{L}{4\kappa Gwt} \tag{2}$$

E and *G* are respectively the Young's and shear modulus of the adherend. $\kappa \approx 5/6$ is the shear correction factor of the beam. From these expressions analytical expressions of the mode I and mode II energy release rate are obtained :

$$G_I = \frac{12a^2P_I^2}{Ew^2t^3} + \frac{P_I^2}{\kappa Gw^2t} \qquad G_{II} = \frac{9a^2P_{II}^2}{16Ew^2t^3} \tag{3}$$

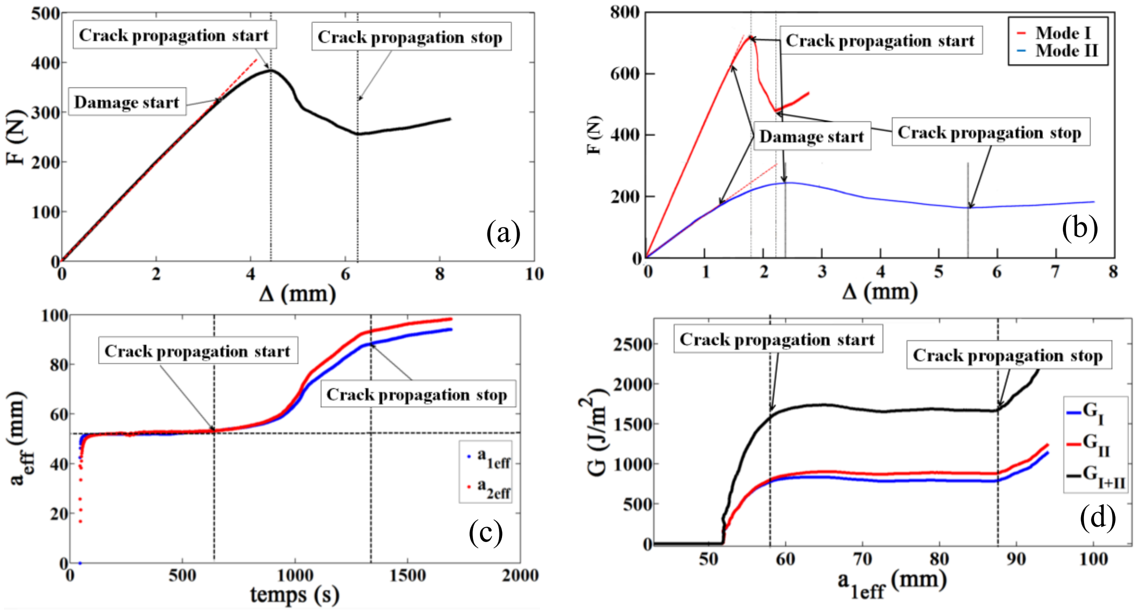

Figure 2. (a) Force versus Displacement evolution, (b) Mode I and Mode II partition. (c) Apparent crack length propagation, (d) apparent energy release rate evolution.

For equal mode I and mode II contribution (viz. $G_I = G_{II}$) we choose $c = 79$mm. Assuming, the shear compliance of the adherend is negligible, and combining equation (2) and (3), a simple expression is obtained which enables to adjust the *c* parameter value for a given expected value of the mode mixity ratio G_I/G_{II}.

$$\frac{G_I}{G_{II}} = \frac{4}{3}\left(\frac{3c - L}{c + L}\right)^2 \tag{4}$$

In Figure 2 are represented the force versus displacement evolution from which are calculated the evolution the apparent crack length as deduced for the mode I an mode II compliances (equations 2) so as the evolution of mode I and mode II energy release rate along the crack propagation. These results indicates that the crack propagates a stable manner but during a short period compared to the total experiment duration. During the crack propagation, apparent G_I and G_{II} values remain stable $G_I \approx G_{II} \approx 750\text{J.m}^{-2}$.

BEAM ON ELASTIC FOUNDATION ANALYSIS

The standard SBT analysis of fracture mechanics analysis can be improved by taking into account the influence of the interface compliance as generally done with the root correction corrections methods. Assuming the interface or bondline behaviour is linear elastic, thin and plane strain conditions, the constitutive equations reduce to two uncoupled fourth order differential equations in σ (peel stress) and τ (shear stress) :

$$0 = \frac{t_a}{E_a^*}\frac{d^4\sigma}{dx^4} - 2\frac{w}{\kappa GS}\frac{d^2\sigma}{dx^2} + \frac{2w}{EI}\sigma \tag{5}$$

$$0 = -\frac{t_a}{G_a}\frac{d^3\tau}{dx^3} + 2w\left[\frac{1}{EI}\left(\frac{t}{2}\right)^2 + \frac{1}{ES}\right]\frac{d\tau}{dx} \tag{6}$$

two wave number are found which controls the extension of the process zone (high stress gradient) near the crack tip :

$$\lambda_\tau = \sqrt{\frac{2wG_a}{t_a}\left(\left(\frac{t}{2}\right)^2\frac{1}{EI} + \frac{1}{ES}\right)} \tag{7}$$

$$\lambda_{\sigma i} = \lambda\sqrt{2\left(\mu \pm \sqrt{\mu^2 - 1}\right)} = \lambda.\alpha_i \tag{8}$$

with :

$$\lambda = \frac{\sqrt{2}}{2}\left(2w\frac{E_a^*}{t_a}\frac{1}{EI}\right)^{1/4} \tag{9}$$

$$\mu = \frac{\sqrt{2w\frac{E_a^*}{t_a}EI}}{\kappa GS} \tag{10}$$

The process zone is difficult to investigate by using only the macroscopic force versus displacement evolution. Indeed, the sensivity of these experimental data to the shape of the law is poor [7]. Furthermore many experimental artefact corrupt the measured data. For finer investigation, digital image correlation technique is used to vizualize the displacement field of the specimen in the vicinity of the crack tip.

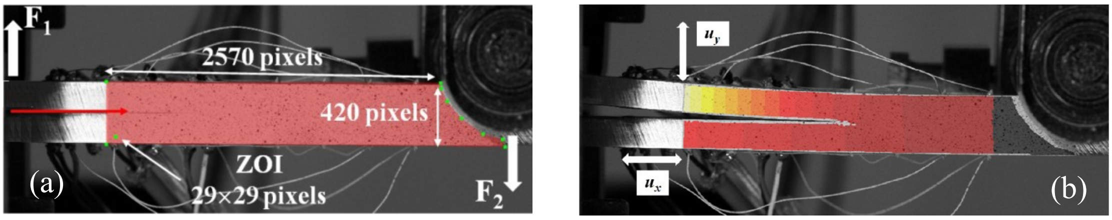

Figure 3. (a) Zone of Interest for DIC analysis, (b) Vertical displacement field, as image with DIC.

The side of the specimen along the crack path is observed with a Canon EOS 400D digital camera (Canon Inc., Tokyo, Japan) equipped with a macro object. 10,1 Mega-Pixel gray scale images are acquired to observe the crack propagation and the specimen deformation. For finer measurement of the deformation of the adherend and of the crack opening and sliding, digital image correlation analysis are performed with VIC-2D software (Correlated Solutions, Inc., Columbia, USA). For proper analysis the observed surface should have random texture with high contrast. To obtain such a pattern, the side of the specimen is first painted in white then black paint is sprayed so that fine drops are randomly deposited (See Figure 3(a)).

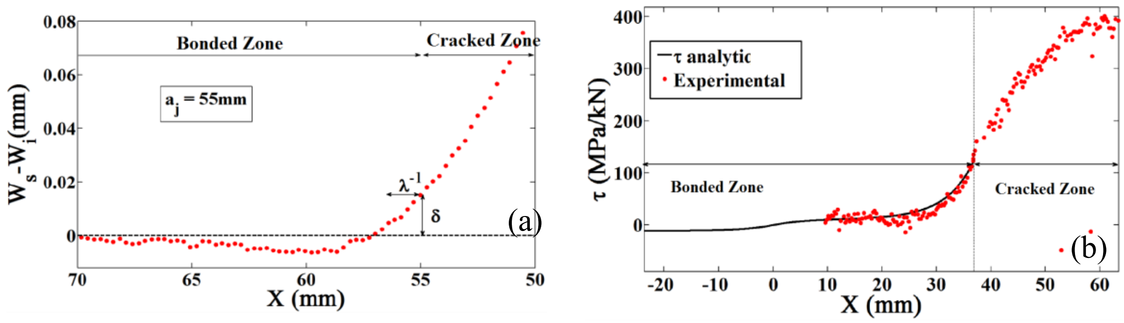

Figure 4. (a) Normal displacement jump across the interface, (b) Comparison between theoretical shear stress calculated with MMB elastic model and DIC measurement of horizontal displacement jump across the interface.

In Figure 4 are presented the results of DIC measurements at two instants of the crack propagation. Two separate the mode I and mode II (viz. peel and shear) contributions, the normal and tangential displacements along both sides of the interface are extracted and then substracted. The interface normal and horizontal displacement discontinuity when crossing the interface is found and compared to results found with the model. A exponential attenuation of the displacement discontinuity at the vicinity of the crack tip is found which is similar to the one predicted with the elastic model. With this analysis the parameters $\lambda_\sigma^{-1} \approx 65$mm $\lambda_\tau^{-1} \approx 12$mm are found.

BACKFACE STRAIN MONITORING

The DIC measurements have been successfully used to measure the deformation of the specimen under mixed mode loading and estimate the interface compliance through the parameters λ_σ and λ_τ. However, a non-linear adhesive behaviour was expected which is not visible on the DIC measurement due to poor sensitivity. For finer investigation of the cohesive forces distribution, backface strain measurement is used. Is consists in measuring the evolution of the adherend upper and lower skin strain during the crack propagation. In the MMB test, two strain gages must be bonded to the specimen at the same position in order to distinguish the mode I and mode II contribution. In the present experiment, 8 strain gauges (Vishay Micro-Measurements reference EA-13-060LZ-120/E with 120Ω nominal resistance and 2 mm grid size) are used they are placed at [55 63 71 79] mm from the right support. With the elastic model, assuming there is no interaction between the process zone and the specimen supports, the difference of the strain signals, $\Delta\varepsilon$, and the sum, $\Sigma\varepsilon$, of the strain signals measured on the lower and upper adherend are given by relations :

$$\Delta\varepsilon(x)/2 \approx -s\frac{t}{2}\frac{P_{II}}{EI}\left\{\frac{3}{2}a - \frac{x}{2} - \frac{a}{2}.exp(\lambda_\tau x)\right\} \tag{11}$$

$$\Sigma\varepsilon(x)/2 \approx \frac{t}{2}P_I\big(\lambda_1 C_1 exp(\lambda_1 x) + \lambda_2 D_1 exp(\lambda_2 x)\big) \tag{12}$$

with :

$$C_1 = \left(\lambda_1 - \frac{k_b}{\kappa GS}\frac{1}{\lambda_1}\right)A_1 \qquad D_1 = \left(\lambda_2 - \frac{k_b}{\kappa GS}\frac{1}{\lambda_2}\right)B_1 \tag{13}$$

And :

$$A_1 = \frac{a^3}{4EI_b}\frac{\alpha_1}{(\lambda a)^3}\left\{\frac{4\lambda a - \alpha_2^3 + 4\mu\alpha_2}{\alpha_1^3 - \alpha_2^3 + 4\mu(\alpha_2 - \alpha_1)}\right\} \tag{14}$$

$$B_1 = \frac{a^3}{4EI_b}\frac{\alpha_2}{(\lambda a)^3}\left\{\frac{4\lambda a - \alpha_1^3 + 4\mu\alpha_1}{\alpha_2^3 - \alpha_1^3 + 4\mu(\alpha_1 - \alpha_2)}\right\} \tag{15}$$

Schematicaly, it confirms that the $\Delta\varepsilon$ evolution is sensitive to the shear cohesive forces distribution while the $\Sigma\varepsilon$ evolution [11, 12, 13]. These evolution are plotted as the function of the instantaneous crack length which is determined for compliance measurements and using equations 2, as seen in Figure 5. This measurements are compared with equations 11 and 12. It reveals a λ_σ and τ_λ controlled region but, the difference with the elastic model also indicates with a better sensitivity the presence of interface nonlinearity.

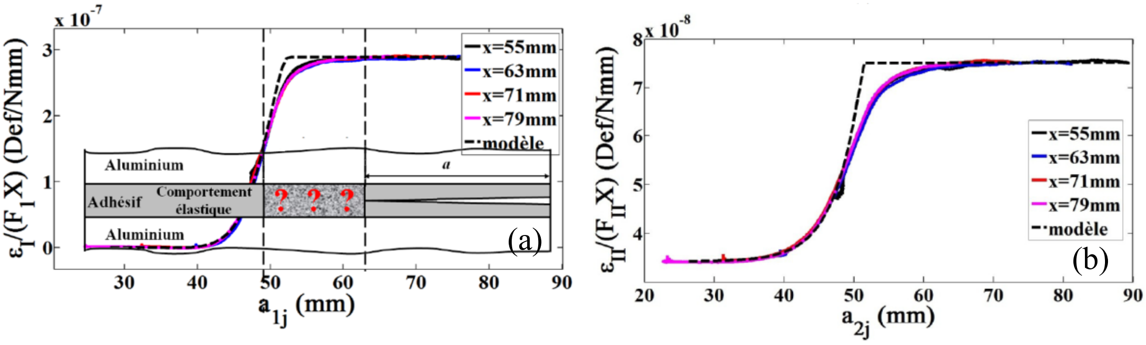

Figure 5. (a) Zone of Interest for DIC analysis, (b) Vertical displacement field, as image with DIC.

CONCLUSIONS

A combined analytical and experimental analysis of mixed mode crack propagation with the MMB test has been proposed. It indicates that a simple elastic model is sufficient for analyzing the experiment with classical analysis technique or when using DIC technique. For finer investigation of the cohesive force distirbution in the process zone, backface monitoring technique should be used, which allow to reveal non linear effect at the bondline scale.

REFERENCES

1. Barroso, A. , Paris, F., Mantic, V. (2009), Compos. Sci. and Technol. **69**, 1746-1755
2. Rippling, E.J., Mostovoy, S., Patrick, R.L. (1964), Mater. Res. Stand., 129–134
3. de Morais, A.B. , Pereira, A.B. (2006), Compos. Sci. and Technol., **66**, 1889-1895
4. Zhang, J., Peng, L., Zhao, L., Fei, B. (2012), Int. J. Fatigue, **40**, 7-15.
5. Borg, R., Nilsson, L., Simonsson, K. (2004), Compos. Sci. and Technol. **64**, 269-278
6. Khoramishad, H., Crocombe, A.D., Katnam, K.B., Ashcroft, I.A. (2010), Int. J. Fatigue, **32,** No 7, 1146-1158.
7. Alfano, G. (2006), Compos. Sci. and Technol., **66**, No 6, 723-730.
8. Sørensen, B.F., Jacobsen, T.K. (2003), Eng. Fract. Mech., **70**, No 14, 1841-1858.
9. Sørensen, B.F., Jacobsen, T.K. (2003), Compos. Sci. and Technol., **69**, No 3-4, 445-456.
10. Ji, G., Ouyang, Z., Li, G. (2012), Mech Mater, **47**, 24-32
11. Ben Salem, N., Budzik, M.K., Jumel, J., Shanahan, M.E.R. (2013), Eng. Fract. Mech., In Press
12. Budzik, M.K., Jumel, J., Ben Salem, N., Shanahan, M.E.R. (2013), Int. J. Solids Struc., **50**, No 2, 310-319.
13. Budzik, M.K., Jumel, J., Shanahan, M.E.R. (2011), Theor. Appl. Fract. Mec., **56**, No 1, 310-319.